

Maximum asymmetry in strain induced mechanical instability of graphene: Compression versus tension

Yu Zhang and Feng Liu

Citation: *Appl. Phys. Lett.* **99**, 241908 (2011); doi: 10.1063/1.3666856

View online: <http://dx.doi.org/10.1063/1.3666856>

View Table of Contents: <http://apl.aip.org/resource/1/APPLAB/v99/i24>

Published by the [American Institute of Physics](http://www.aip.org).

Related Articles

Axial and lateral lattice strain states under a tensile load in as-reacted and prebent CuNb/Nb₃Sn wires using neutron diffraction

J. Appl. Phys. **111**, 043908 (2012)

Electronic structures of silicene fluoride and hydride

Appl. Phys. Lett. **100**, 083102 (2012)

Field-induced changes in polarization and magnetization in Tb_{0.3}Dy_{0.7}Fe₂/PZT laminate composite

J. Appl. Phys. **111**, 043906 (2012)

Strain relaxation analysis of LaAlO₃/SrTiO₃ heterostructure using reciprocal lattice mapping

Appl. Phys. Lett. **100**, 071901 (2012)

Bending of metal-filled carbon nanotube under electron beam irradiation

AIP Advances **2**, 012142 (2012)

Additional information on *Appl. Phys. Lett.*

Journal Homepage: <http://apl.aip.org/>

Journal Information: http://apl.aip.org/about/about_the_journal

Top downloads: http://apl.aip.org/features/most_downloaded

Information for Authors: <http://apl.aip.org/authors>

ADVERTISEMENT



HAVE YOU HEARD?

Employers hiring scientists
and engineers trust
physicistodayJOBS



<http://careers.physicistoday.org/post.cfm>

Maximum asymmetry in strain induced mechanical instability of graphene: Compression versus tension

Yu Zhang and Feng Liu^{a)}

Department of Materials Science and Engineering, University of Utah, Salt Lake City, Utah 84112, USA

(Received 31 October 2011; accepted 16 November 2011; published online 15 December 2011)

We demonstrate that graphene, as the thinnest possible solid membrane of only one atomic layer thick, exhibits the maximum asymmetry in tensile versus compressive strain induced mechanical instability. Using continuum mechanics analysis and molecular dynamics simulations, we show that for graphene nanoribbons (sheets) with a typical length (size) of ~ 100 nm, the critical compressive strain for buckling instability is only $\sim 10^{-4}\%$, while the critical tensile strain for fracture is $\sim 2\%$, a four orders of magnitude difference. Such a large asymmetry implies that practically, strain engineering of graphene devices is only viable with application of tensile strain but difficult with compressive strain. © 2011 American Institute of Physics. [doi:10.1063/1.3666856]

Strain engineering, a strategy being widely used in semiconductor devices,¹ has recently been proposed to change the electrical properties of graphene and graphene nanopatterns² for potential application in future graphene-based electronics. Strain has been shown to modulate the electronic,^{3–7} magnetic,⁸ and transport properties^{2,9–11} of graphene. In general, theoretical studies are based on the assumption that the planar structure of graphene and graphene nanoribbons (GNRs) remain stable under the applied strain so that the effect of strain is independent of the sign of strain;^{2–7} i.e., a tensile or compressive strain induces the same effect. Such an assumption, however, can be rather unrealistic, because graphene was theoretically predicted to undergo mechanical instability under strain,^{12,13} and recent experiments^{14,15} showed direct evidence of buckling (or rippling) of graphene as a result of thermal strain. Since the out-of-plane undulation and fracture may invalidate some flat-graphene strain theories, it is important to understand the mechanical instability of graphene against out-of-plane undulation and fracture induced by strain, especially the role played by the sign of strain, compression versus tension.

We may ask the general question of how the mechanical instability of a thin film will depend on the sign of strain. Under tension, the film will eventually break, creating two fracture surfaces. The critical tensile strain (ϵ_{cr}^t) for fracture can be simply obtained by equaling the strain energy to the energy of two fracture surfaces, i.e., $(1/2)ALE\epsilon_{cr}^2 = 2A\gamma$, where A is the area of cross section, L is the length along which the uniaxial tension is applied, E is the Young's modulus, and γ is the surface energy. Thus, $\epsilon_{cr}^t \sim 2\sqrt{\gamma/EL}$, which does not depend on the film thickness. In contrast, compression may induce two types of instability: fracture and buckling. For very thick film, the critical compressive strain for fracture is comparable to the critical tensile strain for fracture. For very thin films, however, the compressive strain will first induce buckling preempting fracture. The critical compressive strain (ϵ_{cr}^c) for the buckling instability is determined by the competition between bending energy of $1/2B\kappa^2A$ and stretching energy $1/2Et\epsilon m^2A$, where $B \sim Et^3$ is the bending modulus, t is the thickness, κ and m

are curvature and slope due to out-of-plane deformation. Thus, $\epsilon_{cr}^c \sim t^2$, which shows a strong dependence on the film thickness, i.e., a thinner film is easier to buckle.

The above analysis implies a high asymmetry in compressive versus tensile strain induced mechanical instability in thin films as the film thickness is reduced. If the film is thick towards the bulk limit, the critical strain is the same for both compression and tension. If the film is thin, however, compression induces buckling first so that the critical strain for compression is smaller than for tension and the difference increases with the decreasing film thickness. Naturally, graphene, as the thinnest film possible of only one atomic layer thick, is expected to exhibit the maximum asymmetry in compressive versus tensile strain induced mechanical instability.

To quantify the asymmetry of strain induced mechanical instability in graphene, we have performed continuum mechanics calculations and molecular dynamics (MD) simulations to investigate different forms of mechanical deformation of graphene induced by uniaxial and biaxial compressive and tensile strain. We first consider the case of narrow GNRs (Refs. 12 and 16) under uniaxial strain along its length direction, as shown in Fig. 1. Its mechanical instability is manifested in the form of bucking under compression and fracture under tension (see two schematic insets in Fig. 1). Under compressive strain (ϵ^c), the total strain energy can be calculated from continuum mechanics theory which consists of a bending and a stretching term as¹³

$$U_{total} = B/2 \int_A (\partial^2 \zeta / \partial x^2)^2 dA + Et/2 \int_A \epsilon^c (\partial \zeta / \partial x)^2 dA, \quad (1)$$

where $\zeta(x)$ is the out-of-plane displacement at point x along the ribbon. Using variational method and periodic boundary condition, energy minimization leads to the critical compressive strain for buckling instability:^{13,17}

$$\epsilon_{cr}^c = \frac{\pi^2 t^2}{3(1-\nu^2)L^2}. \quad (2)$$

where ν is the Poisson ratio and L and t are the length and thickness of the GNR, respectively. The critical tensile strain for fracture, as discussed above, is

^{a)}Electronic mail: fliu@eng.utah.edu.

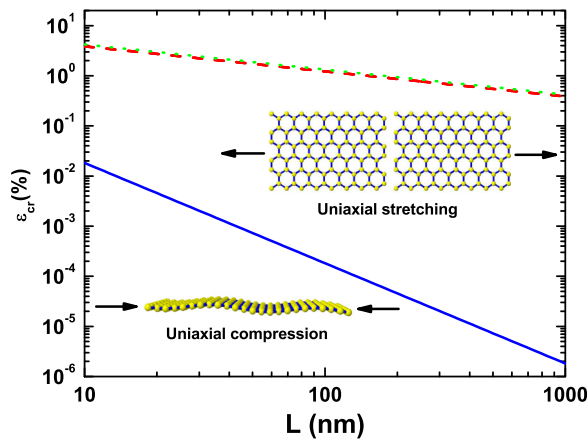


FIG. 1. (Color online) Critical strain for mechanical instability in narrow GNRs: compression induced buckling versus tension induced fracture. Solid blue, dashed red, and dot green lines indicate uniaxial compression, uniaxial stretching along zigzag direction, and uniaxial stretching along armchair direction, respectively.

$$\varepsilon_{cr}^t \sim 2\sqrt{E_{edge}/EtL}. \quad (3)$$

Here, E_{edge} is the edge energy of GNR. Using $E = 4.27$ TPa, $\nu = 0.19$, and $t = 0.7$ Å (Ref. 18) and edge energies of armchair edge = 1.0 eV/Å and zigzag edge = 1.2 eV/Å (Ref. 12), we plot ε_{cr}^c and ε_{cr}^t as a function of L in Fig. 1. We also derived ε_{cr}^c and ε_{cr}^t from MD simulations,¹⁸ which show very good agreement with the analytical results (see Fig. 3 below).

Figure 1 shows a significant difference in ε_{cr}^c and ε_{cr}^t . For L from 10 to 1000 nm, $\varepsilon_{cr}^c \sim L^{-2}$, varies from 0.02% to 2×10^{-6} %, while $\varepsilon_{cr}^t \sim L^{-1/2}$, varies from 5% to 0.5%. For GNRs with a typical length of ~ 100 nm, ε_{cr}^c for buckling instability is four orders of magnitude smaller than ε_{cr}^t for fracture, signifying a maximum asymmetry in strain induced mechanical instability with respect to the sign of strain. The GNRs are extremely unstable against compressive strain; even $\sim 0.02\%$ compressive strain will cause buckling of a 10-nm-long GNR. This can be understood in relation to pressure induced buckling shape transition in carbon nanotubes,^{18,19} both are caused by the same fact that the energy cost to change (or compress) C–C bond length is about two orders of magnitude higher than that to change (or bend) bond angle.¹⁹

The results in Fig. 1 set the thermodynamic limits of critical strain for mechanical instability in GNRs. Their values may be slight different if different force-fields are used¹⁷ and be modified by kinetic conditions, meta-stability, nonlinear elasticity, and strain rate in real experiments. For example, experiments have observed graphene sustains up to even 25% stretching without fracture.²⁰ However, the maximum asymmetry between the compressive strain induced buckling versus tensile strain induced fracture should remain valid. The fact that a GNR can only maintain its planar structure for a tiny amount of compressive strain has an important practical implication. It means that strain engineering is very unlikely with the application of compressive strain, because as soon as the GNR buckles, it relieves the applied compressive strain, mitigating any useful electronic effects associated with the compressive strain. One may consider putting the GNR onto a

substrate to suppress the buckling instability so that larger compressive strain can be applied. But then, one has to consider the effect of interface on the electronic properties of GNRs in addition to strain.

For a narrow GNR whose width is very small, fracture is the only dominant form of mechanical instability occurs under uniaxial tensile strain along the length direction, as shown above, i.e., the tensile strain causes the GNR to stretch its length until fracture. However, for a wide GNR, another form of mechanical instability may occur with buckling in the width direction orthogonal to the direction of the uniaxial tensile strain being applied, as shown by the inset in Fig. 2. This interesting form of instability has been predicted for ultrathin solid membrane²¹ and observed in graphene.^{14,15} This can be qualitatively understood in terms of Poisson effect, as stretching along the length direction (say x -direction) will cause compression in the orthogonal width direction (y -direction) which then induces buckling along the y -direction. The strain relation is $\varepsilon_{yy} = -\nu\varepsilon_{xx}$, and the total energy in this case [different from Eq. (1)] has an additional term of stretching energy in the y -direction

$$U_{total} = B/2 \int_A (\partial^2 \zeta / \partial x^2)^2 dA + Et/2 \int_A \varepsilon^t (\partial \zeta / \partial y)^2 dA - Et/2 \int_A \varepsilon^t (\partial \zeta / \partial y)^2 dA, \quad (4)$$

where $\zeta(x, y)$ is the out-of-plane displacement at point (x, y) . Variation of total energy in Eq. (4) leads to the following differential equation:

$$B(\partial^4 \zeta / \partial y^4) - tE\varepsilon_{x0}(\partial^2 \zeta / \partial x^2) + (L/W)E\nu\varepsilon_{x0}(\partial^2 \zeta / \partial y^2) = 0. \quad (5)$$

Solving Eq. (5), we obtain the critical strain for the y -direction buckling orthogonal to the x -direction tensile strain as

$$\varepsilon_{cr}^t = \frac{\pi^2 t^2}{3(1-\nu^2)W^2[\nu - (W/2L)^2]}; \quad W < 2\sqrt{\nu}L. \quad (6)$$

Comparing Eq. (6) (uniaxial tension) with Eq. (2) (uniaxial compression), we can see that if the length L , along which the strain is applied, was infinite long, the critical strain for the two cases will have the same form, differing only by a

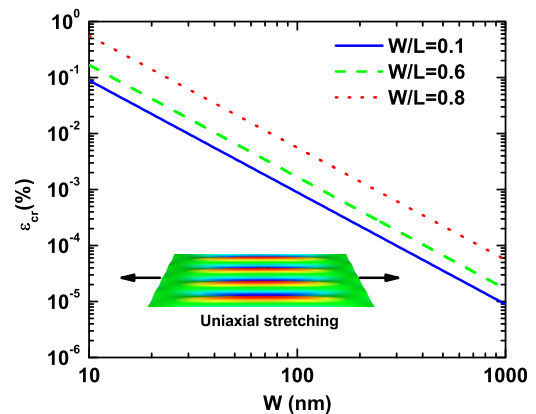


FIG. 2. (Color online) Critical tensile strain for uniaxial stretching induced orthogonal buckling for three different width-to-length ratios of wide GNRs.

factor of ν . Figure 2 plots the critical tensile strain for the “orthogonal” buckling instability due to uniaxial stretching, using three different aspect ratios (W/L). ϵ_{cr}^t , in this case, decreases from 0.1–0.5% to $1\text{--}5 \times 10^{-5}\%$ with increasing width (W), which are about one magnitude larger than ϵ_{cr}^c shown in Fig. 1, reflecting the Poisson effect. So, the asymmetry in compressive versus tensile strain induced mechanical instability both in the buckling form in a wide GNR is much smaller than that in a narrow GNR where compressive and tensile strain induces respectively buckling and fracture instability.

Lastly, we consider the case of 2D graphene sheet. For simplicity, we assume the graphene sheet with two zigzag (x -direction) and two armchair edges (y -direction). Because graphene is well known to be elastically isotropic, we have the same analytical results as shown in Eq. (2) and Fig. 1 that the critical compressive strain for buckling increases with decreasing length L as L^{-2} . This is further confirmed by MD simulations, as shown in Fig. 3. Similar results were also obtained using different empirical potentials and sometimes difference was made in the choice of graphene thickness.¹⁷

When biaxial compressive strain is applied, the longer side will buckle first and the shorter side will then never buckle if the graphene sheet has a rectangular shape. If, however, the graphene sheet has a nearly squared shape, then buckling may occur simultaneously in both directions, as shown by the inset in Fig. 3. To study buckling instability of 2D graphene sheet under biaxial compression, we use a shape as close as possible to a square. These include sheet dimensions of 12.65 \AA (zigzag edge) \times 13.14 \AA (armchair edge), $25.30 \text{ \AA} \times 26.28 \text{ \AA}$, and $37.95 \text{ \AA} \times 39.42 \text{ \AA}$, and the results are shown in Fig. 3, in comparison with the results of uniaxial compression. The analytical solution of this problem is

$$\epsilon_{x,bi} = \frac{\pi^2 t^2}{3(1-\nu^2)L'^2}, \quad (7)$$

where $L'^{(-2)} = (L_x'^{-2} + L_y'^{-2})/2$ with $L_x \approx L_y$, and Eq. (7) have the same form as Eq. (2). Figure 3 shows that the analytical results agree well with MD simulation results. If biaxial

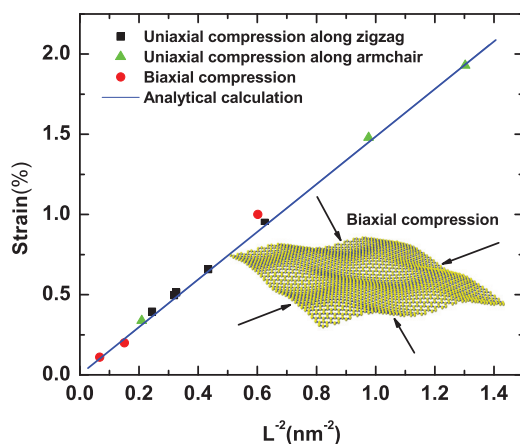


FIG. 3. (Color online) Critical compressive strain versus L^{-2} for buckling of graphene sheet under uniaxial and biaxial strain, obtained from analytical calculations (solid line) and MD simulations (data points).

ial tensile strain is applied, the 2D graphene sheet will fracture above a critical tensile strain, which is defined by the same equation as Eq. (3) but with average edge energies and edge length along the two directions. Then, the 2D graphene sheet will also exhibit the maximum asymmetry in tensile versus compressive strain induced mechanical instability, same as discussed above for narrow GNRs.

We note that for GNRs, the intrinsic non-zero edge stress may also induce localized edge rippling instability,¹² without externally applied strain. Thus, there can be interplay between the applied strain induced rippling and the intrinsic edge stress induced rippling in GNRs, which modifies the critical strains we derive. However, the general physical picture of the strained induced instability, especially the point of asymmetry that we emphasize remains correct.

In conclusion, we have studied the mechanical instability of GNRs and graphene sheet under uniaxial/biaxial compressive/tensile strains, using continuum mechanics theory and MD simulations. We demonstrate that the narrow GNRs and 2D graphene sheet exhibit a maximum asymmetry in tensile versus compressive strain induced mechanical instability: the critical compressive strain for buckling is several orders of magnitude smaller than the critical tensile strain for fracture, because of the extreme thinness of graphene with only one atomic layer thickness. This thinness also makes the amount of compressive strain that graphene can sustain to maintain its planar structure to be extremely small, only a hundredth of a percent for a graphene size of 10 nm. These findings have an important practical implication that strain engineering of graphene devices is only viable with application of tensile strain but difficult with compressive strain.

¹Z. Liu, J. Wu, W. Duan, M. G. Lagally, and F. Liu, *Phys. Rev. Lett.* **105**, 016802 (2010).

²V. M. Pereira and A. H. Castro Neto, *Phys. Rev. Lett.* **103**, 046801 (2009).

³M. Topsakal, S. Cahangirov, and S. Ciraci, *Appl. Phys. Lett.* **96**, 091912 (2010).

⁴X. Peng and S. Velasquez, *Appl. Phys. Lett.* **98**, 023112 (2011).

⁵Y. Lu and J. Guo, *Nano Res.* **3**, 189 (2010).

⁶M. Poetschke, C. G. Rocha, L. E. F. Foa Torres, S. Roche, and G. Cuniberti, *Phys. Rev. B* **81**, 193404 (2010).

⁷L. Sun, Q. Li, H. Ren, H. Su, Q. W. Shi, and J. Yang, *J. Chem. Phys.* **129**, 074704 (2008).

⁸N. Levy, S. A. Burke, K. L. Meaker, M. Panlasigui, A. Zettl, F. Guinea, A. H. Castro Neto, and M. F. Crommie, *Science* **329**, 544 (2010).

⁹D. Yoon, Y. Son, and H. Cheong, *Phys. Rev. Lett.* **106**, 155502 (2011).

¹⁰F. Guinea, M. I. Katsnelson, and A. K. Geim, *Nature Phys.* **6**, 30 (2009).

¹¹F. Ding, H. Ji, Y. Chen, A. Herklotz, K. Dorr, Y. Mei, A. Rastelli, and O. G. Schmidt, *Nano Lett.* **10**, 3453 (2010).

¹²B. Huang, M. Liu, N. Su, J. Wu, W. Duan, B. Gu, and F. Liu, *Phys. Rev. Lett.* **102**, 166404 (2009).

¹³Z. F. Wang, Y. Zhang, and F. Liu, *Phys. Rev. B* **83**, 041403(R) (2011).

¹⁴W. Bao, F. Miao, Z. Chen, H. Zhang, W. Jang, C. Dames, and C. N. Lau, *Nat. Nanotechnol.* **4**, 562 (2009).

¹⁵C. Chen, W. Bao, J. Theiss, C. Dames, C. N. Lau, and S. B. Cronin, *Nano Lett.* **9**, 4172 (2009).

¹⁶Q. Yan, B. Huang, J. Yu, F. Zheng, J. Zang, J. Wu, B. Gu, Feng Liu, and W. Duan, *Nano Lett.* **7**, 1469 (2007).

¹⁷Q. Lu and R. Huang, *Int. J. Appl. Mech.* **1**, 443 (2009).

¹⁸J. Zang, A. Treibergs, Y. Han, and F. Liu, *Phys. Rev. Lett.* **92**, 105501 (2004); J. Zang, O. A. Palacios, and F. Liu, *Commun. Comput. Phys.* **2**, 451 (2007).

¹⁹D. Y. Sun, D. J. Shu, M. Ji, F. Liu, M. Wang, and X. G. Gong, *Phys. Rev. B* **70**, 165417 (2004).

²⁰C. Lee, X. D. Wei, J. W. Kysar, and J. Hone, *Science* **321**, 385 (2008).

²¹E. Cerda and L. Mahadevan, *Phys. Rev. Lett.* **90**, 074302 (2003).